Carbohydrate Polymers 264 (2021) 117991

Contents lists available at ScienceDirect

Carbohydrate Polymers

journal homepage: www.elsevier.com/locate/carbpol

Water-soluble polysaccharides from *Pleurotus eryngii* fruiting bodies, their activity and affinity for Toll-like receptor 2 and dectin-1

Christiane Færestrand Ellefsen [a,*], Christian Winther Wold [a], Alistair L. Wilkins [b], Frode Rise [c], Anne Berit C. Samuelsen [a]

[a] Department of Pharmacy, University of Oslo, P.O.Box 1068 Blindern, NO-0316, Oslo, Norway
[b] School of Science and Engineering, University of Waikato, Private Bag 3105, Hamilton, 3240, New Zealand
[c] Department of Chemistry, University of Oslo, P.O.Box 1033 Blindern, NO-0315, Oslo, Norway

ARTICLE INFO

Keywords:
Pleurotus eryngii
β-Glucan
Mannogalactan
TLR-2
Dectin-1

ABSTRACT

The mushroom cell wall contains polysaccharides that can activate cells of the innate immune system through receptors such as Toll-like receptors (TLR) and dectin-1. In the present study, *Pleurotus eryngii* polysaccharide fractions containing a 3-*O* methylated mannogalactan and (1→3)/(1→6)-β-D-glucans were isolated and extensively characterized by 2D NMR and methylation analysis. Traces of a (1→3)-α-D-glucan and a (1→2)-α-D-mannan were also observed. Affinity for TLR2, TLR2-TLR6 and dectin-1 using HEK-cells expressing the relevant receptor genes was tested. PeWN, containing the 3-*O* methylated mannogalactan, was inactive towards TLR2, whereas fraction PeWB, containing more β-glucan, activated the TLR2-TLR6 heterodimer. Activation of the human β-glucan receptor dectin-1 correlated with the amount of β-glucan in each fraction. Nitric oxide and cytokine supernatant levels of D2SC/1 dendritic cells stimulated with the *P. eryngii* fractions and interferon-γ were low to moderate. The results indicate that the immunomodulatory activity of water-soluble *P. eryngii* polysaccharide fractions is modest.

1. Introduction

The king oyster mushroom, *Pleurotus eryngii*, is an edible mushroom native to areas from the western coasts of France and Morocco through Mediterranean regions to Khazakstan and India (Zervakis, Venturella, & Papadopoulou, 2001). Unlike many mushrooms of the *Basidomycetes* phylum, *Pleurotus* species can be cultivated quite easily on a variety of agricultural wastes (Baysal, Peker, Yalinkilic, & Temiz, 2003). This makes them good subjects for studying mushroom molecules and their biological properties. The fungal cell wall consists of polysaccharides such as chitin, glucans and mannans (Hohl, Rivera, & Pamer, 2006). Previous studies have shown that king oyster mushroom contains partially methylated mannogalactans and partially methylated galactans (Abreu et al., 2021; Biscaia et al., 2017; Carbonero et al., 2008; Yan et al., 2019; Zhang, Zhang, Yang, & Sun, 2013). Partially methylated mannogalactans are common in species of the *Pleurotus* genus, and have been isolated from *P. ostreatus* var. *Florida*, *P. ostreatoroseus*, *P. pulmonarius*, *P. geesteranus* and *P. sajor-caju* (Rosado et al., 2003; Silveira et al., 2015; Smiderle et al., 2008; Zhang, Xu, Fu, & Sun, 2013). Studies on the biological activities of these heterogalactans have suggested antitumor, antinociceptive, and anti-inflammatory activity (Biscaia et al., 2017; Silveira et al., 2015; Smiderle et al., 2008). The structures and activities of polysaccharides of *Pleurotus eryngii* are further elaborated in a recently published review by Zhang et al. (2020). This is also discussed in another recent review, along with extraction techniques towards polysaccharides from different *Pleurotus* spp. (Barbosa, dos Santos Freitas, da Silva Martins, & de Carvalho, 2020). Reports have suggested that the methylated mannogalactans from *P. eryngii* have immunoactivating abilities, by activation of macrophages through binding to Toll-like receptor 2 (TLR2) (Yan et al., 2019).

TLR2 is a pattern recognition receptor (PRR) found on various immune cells, and is part of the immune system's defense against microbial invasion, as it recognizes certain molecular patterns on the microbe's surfaces (Murphy & Weaver, 2017; Rock, Hardiman, Timans, Kastelein, & Bazan, 1998). Binding to TLR2 may result in the production of reactive oxygen species (ROS), release of proinflammatory cytokines, or phagocytosis initiation (Medzhitov & Janeway, 2000; Murphy & Weaver, 2017). TLR2 exists as a heterodimer together with either TLR1

* Corresponding author.
E-mail address: c.f.ellefsen@farmasi.uio.no (C.F. Ellefsen).

https://doi.org/10.1016/j.carbpol.2021.117991
Received 21 January 2021; Received in revised form 12 March 2021; Accepted 23 March 2021
Available online 26 March 2021

or TLR6, and activation happens through binding to both components of the heterodimer (Ozinsky et al., 2000; Takeuchi et al., 2002). Known agonists for TLR2-TLR1 are typically triacylated lipopeptides, whereas diacylated lipopeptides bind to and activate TLR2-TLR6 (Takeuchi et al., 2001). Some glycans have also been recognized as TLR2 agonists, for example zymosan, which is a particulate cell wall preparation from *Saccharomyces cerevisiae*, and a known agonist to the TLR2-TLR6 heterodimer (Di Carlo & Fiore, 1958). Its main component is β-glucan, but mannose and protein is also present. The TLR2-binding properties are lost upon removal of the non-β-glucan components, indicating that the β-glucan alone cannot bind to TLR2 (Ikeda et al., 2008).

Dectin-1 is another PRR, and is a c-type lectin found on macrophages, DC, and several other types of immune cells (Willment et al., 2005). This receptor recognizes and binds (1→3)- and (1→6)-β-D-glucans (Brown & Gordon, 2001). Activation of dectin-1 may lead to cytokine release, phagocytosis and production of ROS (Brown et al., 2003; Goodridge et al., 2011). Zymosan binds to and activates dectin-1 due to its β-glucan components (Brown & Gordon, 2001). Particulate β-glucans have been shown to act as dectin-1 agonists, while soluble β-glucans have been suggested to act as dectin-1 antagonists (Goodridge et al., 2011). However, recent reports indicate that although this seems to be the case with mouse dectin-1, human dectin-1 may also be activated by soluble β-glucans (Takano et al., 2017).

Another receptor that is associated with the immunomodulatory activity of β-glucans is the integrin dimer CD11b/CD18 commonly referred to as complement receptor 3 (CR3). CR3 has been shown to work alongside dectin-1 in response to β-glucans, as it responds to smaller, soluble β-glucan fragments (Hong et al., 2004). Studies have also indicated that CR3 is essential for initiating phagocytosis in response to soluble and particulate β-glucans in neutrophils and monocytes (Bose et al., 2013; Bruggen et al., 2009).

β-glucans have been isolated in water-soluble *P. eryngii* fractions previously, both alone and in association with the mannogalactans described above (Abreu et al., 2021; Carbonero et al., 2006; Ma et al., 2014; Synytsya et al., 2009; Yan et al., 2019). Examination of the biological activity of crude *P. eryngii* polysaccharide extracts containing β-glucan have indicated anti-inflammatory effects in mice, possibly mediated through anti-dectin-1 activity (Vetvicka et al., 2019). A joint activation of the two receptors TLR2 and dectin-1 has been proposed to enhance the inflammatory response of immune cells, and has shown a synergistic effect in TNF-α production by human macrophages (Ferwerda, Meyer-Wentrup, Kullberg, Netea, & Adema, 2008; Gantner, Simmons, Canavera, Akira, & Underhill, 2003; Willcocks, Offord, Seyfert, Coffey, & Werling, 2013; Yadav & Schorey, 2006). A combined TLR2 and dectin-1 activation may therefore be a possibility. Furthermore, it has not previously been reported which of the two heterodimers, TLR2-TLR1 and TLR2-TLR6 is involved in the TLR2 activation. Considering structural likeness to zymosan, TLR2-TLR6 seemed the likely candidate. We thus hypothesized that the water-soluble polysaccharides, methylated mannogalactan and associated β-glucans of *P. eryngii* have immunoactivating abilities, acting through TLR2-TLR6 and dectin-1.

2. Methods

2.1. Introduction

Fresh fruiting bodies of *Pleurotus eryngii*, cultivated under sterile conditions, were purchased from Trøndersopp (Verdal, Norway, www.trondersopp.no) and identified by Prof. Klaus Høiland at the Section for Genetics and Evolutionary Biology, University of Oslo. The fruiting bodies were lyophilized and milled before being submitted to extraction.

2.2. Extraction and purification

Lyophilized, milled *P. eryngii* fruiting bodies (150 g) were extracted in several steps as shown in Fig. 1. Firstly, the material was extracted twice with 2000 mL dichloromethane (DCM) by gently stirring at ambient temperature for 20 h, for removal of lipophilic substances. The residue was then subjected to Soxhlet extraction with ethanol until clear extraction solvent, to remove low molecular weight polar substances. Finally, the residue was extracted twice with 2400 mL boiling water under reflux for 5 h. The water extract was treated with 500 mg porcine pancreatin (Sigma-Aldrich, St. Louis, MO, USA) for 3 h at 40 °C, before polysaccharides were precipitated by addition of three volumes of ethanol. The precipitate was washed thrice with 70 % ethanol before dialysis (Mw cut-off 12−14 kDa, SpectraPor® Dialysis membrane, Spectrum Chemical Mfg. Corp., New Brunswick, NJ, USA) and lyophilization.

2.3. Anion exchange chromatography

Anion exchange chromatography was performed on a DEAE Sepharose fast flow column (550 mL, Pharmacia) preloaded with NaCl and coupled to a Pharmacia FPLC system. PeW (200 mg) was dissolved in 50 mL water, filtered and loaded onto the column. A neutral fraction (PeWN) was eluted with water, at a flow rate of 1 mL/min. Further elution was performed using a NaCl gradient (0.0–1.0 M) at a 1 mL/min flow-rate, with 5 mL fractions being collected on a fraction collector. Based on the carbohydrate elution profile, determined by the phenol/sulphuric acid assay (DuBois, Gilles, Hamilton, Rebers, & Smith, 1956), two acidic fractions, PeWA (fractions 70–100) and PeWB (fractions 100–140), were isolated. Fractions were submitted to dialysis (Mw cut-off 12−14 kDa), and freeze-dried.

2.4. Monosaccharide composition

Monosaccharide compositions was determined through methanolysis and subsequent TMS derivatization, as previously described (Nyman, Aachmann, Rise, Ballance, & Samuelsen, 2016). The derivatives were analyzed by capillary gas chromatography, with FID detection. A Restek Rtx-5 silica column (30 m, i.d. 0.25 mm, 0.25 μm film thickness) which was coupled to a Focus GC (Thermo Scientific, Waltham, MA, USA) using split (1/10) injector at constant pressure mode. The temperatures at the injector and detector were 250 °C and 300 °C respectively. The column temperature was 140 °C at the time of injection, and was increased to 150 °C with 1 °C/min, and held there for 3 min before a further increase by 3 °C/min to 170 °C, where it was held for 5 min and then raised to 310 °C by 15 °C/min. The temperature was kept at 310 °C for three minutes. Helium was the carrier gas, and chromatograms were obtained and analyzed with Chromelion software v.6.80 (Dionex Corporation, Sunnyvale, CA, USA). The total carbohydrate content of the fractions PeWN, PeWA and PeWB was determined using the phenol/sulfuric acid assay (DuBois et al., 1956), using a D-glucose standard curve and absorbance measurement at 490 nm.

2.5. Molecular weight determination – SEC-MALLS

The weight-average molecular weight (M_w) of each fraction was determined through size-exclusion chromatography with multi-angle laser light scattering detection (SEC-MALLS) as previously described (Nyman et al., 2016). In brief, carbohydrate samples were analyzed on a serially connected guard-column (Tosoh PWXL) and two size-exclusion columns (Tosoh TSK-gel G6000 PWXL and G6000PWXL) and eluted with 0.1 M sodium nitrate/0.02 % azide solution at 0.5 mL/min from a Shimadzu LC-20HPLC system. A Dawn Helios + 8 eight angle light scattering detector (MALLS) along with a Viscostar II viscometer and an Optilab T-rex RI detector (Wyatt, California, USA) was used for detection, and raw data were collected and processed with Astra software version 6 (Wyatt, USA). The analysis was performed at Nofima, the Norwegian Institute of Food, Fisheries and Aquaculture Research, Ås, Norway.

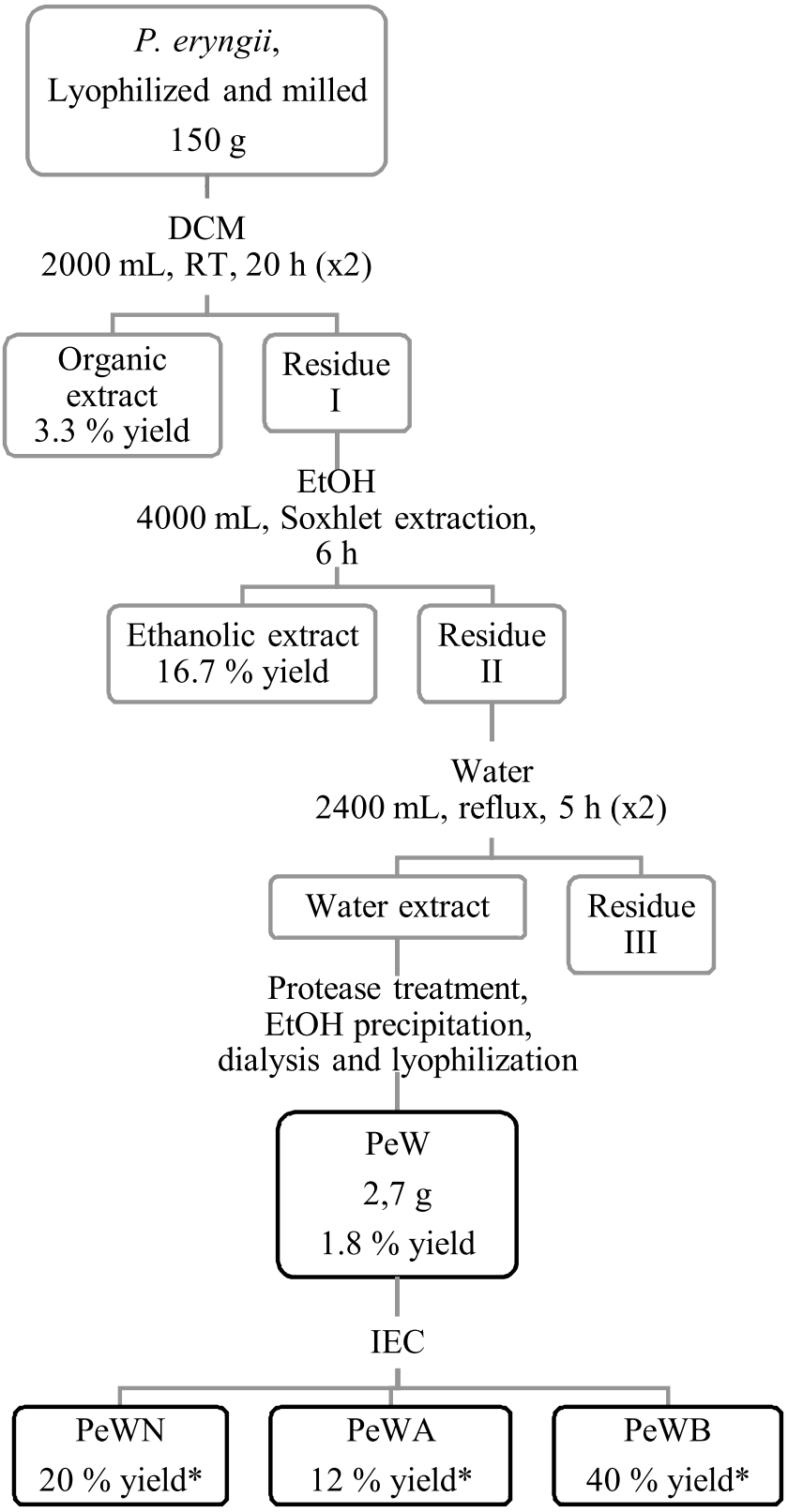

Fig. 1. Flowchart showing the extraction procedure towards water-soluble polysaccharides from *P. eryngii*. *yield from water extract (PeW) dry weight. IEC = ion exchange chromatography.

2.6. Linkage analysis

Methylation, and subsequent hydrolysis, reduction and acetylation was performed as described by Pettolino, Walsh, Fincher, and Bacic (2012), and followed by analysis on a GC–MS-QP2010 (Shimadzu Corporation, Kyoto, Kyoto, Japan) using a Restek Rxi-5MS silica column (30 m, i.d. 0.25 mm, 0.25 μm film thickness) with split injection at constant pressure mode. Initial flow was 1 mL/min, interface temperature was

280 °C, and at the time of injection, the column temperature was 80 °C. After 5 min, the temperature was increased with 10 °C/min to 140 °C, and then by 4 °C/min to 210 °C, and finally by 20 °C/min to 310 °C, where it was kept for 4 min. Helium was used as carrier gas, and the temperature of the ion source was 200 °C. Spectra were analyzed using GC–MS solution software, v.2.10 (Shimadzu Corporation).

2.7. NMR

The samples (approx. 10 mg) were dissolved in 550−600 μL 99.9 % D_2O (Chiron, Trondheim, Norway) and 3-(trimethylsilyl) propionic 2,2,3,3-d_4 acid (TSP, 1 μL, 5 % in D_2O, Sigma-Aldrich) was added as reference. The samples were analyzed on a Bruker Avance III HD 800 MHz spectrometer equipped with 5-mm cryogenic CP-TCI z-gradient probe (Bruker, Billerica, MA, USA). The following experiments were obtained using TopSpin 3.5.5, at 55 °C with or without CW presaturation for suppression of water signals: ^{1}H, ^{13}C, COSY (cosygpprqf, TD(F2) 2048, TD(F1) 512, NS 16, expt 5 h, aq. time 0.11 s), DIPSI2 (dipsi2phpr, TD(F2) 2048, TD(F1) 512, NS 8, expt 1 h, aq. time 0.10 s, 60 ms mixing time), ROESY (roesyphpr, TD(F2) 2048, TD(F1) 256, NS 16, expt 2 h, aq. time 0.11 s), HSQC (awhsqcedetgpsisp2.3−135pr, TD(F2) 2048, TD(F1) 512, NS 8, expt 2 h, aq. time 0.11 s), HMBC (awhmbcgplpndqfpr, TD(F2) 2048, TD(F1) 512, NS 8, expt 2 h, aq. time 0.11 s), and H2BC (h2bcetgpl3, TD(F2) 2048, TD(F1) 512, NS 16, expt 4 h, aq. time 0.13 s). Spectra were processed and analyzed using TopSpin 3.6.2.

2.8. HEK-Blue™ reporter cell lines

HEK-Blue™ hTLR2, hTLR2-TLR6, hDectin-1a and Null1 cells (InvivoGen, Toulouse, France, www.invivogen.com) were grown and maintained according to the description provided by the manufacturer. Cells were maintained in Dulbecco's modified Eagle's medium (DMEM, Life Technologies, Paisley, UK) supplemented with 10 % (v/v) fetal bovine serum (FBS, Sigma-Aldrich), 100 U/mL penicillin, 100 μg/mL streptomycin (Sigma-Aldrich), 100 μg/mL Normocin™ (InvivoGen), and 1X HEK-Blue™ Selection (InvivoGen), 1X HEK-Blue™ CLR Selection (InvivoGen) or Zeocin™ (InvivoGen).

The samples PeWN, PeWA and PeWB (100, 10, 1 μg/mL final concentrations, 20 μL) were added to 96-well plates. Pam2CSK4 (100, 10 or 1 ng/mL, 20 μL, InvivoGen), Pam3CSK4 (100, 10 or 1 ng/mL, 20 μL, InvivoGen), lipopolysaccharide (LPS) (1, 0.5, or 0.1 μg/mL, 20 μL, ultrapure from *Escherichia coli* 0111:B4, Invivogen), laminarin (100 or 60 μg/mL, 20 μL, from *Laminaria digitata*, Sigma-Aldrich), zymosan A (100, 10 or 1 μg/mL, 20 μL, Sigma-Aldrich) and zymosan depleted (100 or 10 μg/mL, 20 μL, InvivoGen) were included as controls. TNF-α (100 ng/mL, 20 μL, Thermo Fischer) was included as a positive control with the null cells. Cells were harvested with PBS or 0.08 % trypsin-EDTA (Sigma-Aldrich) in PBS, and suspended in HEK-Blue™ Detection medium (InvivoGen) to a concentration of 2.8×10^5 cells/mL. To each well, 180 μL cell suspension was added, giving a total of 5×10^4 cells per well. The plates were placed in a humid incubator with 5 % CO_2 at 37 °C for 16 h. Activation was determined through absorbance reading at 635 nm. The experiments were carried out three times, in triplicates.

2.9. NO detection assay

Mouse derived dendritic cells (D2SC/1, a gift from Alexandre Corthay, Oslo University Hospital) were grown and maintained in DMEM supplemented with 4.5 g/L glucose, 10 % (v/v) fetal bovine serum, 100 U/mL penicillin, 100 μg/mL streptomycin, 1 % Na-pyruvate, and 500 μL 2-mercaptoethanol. Cells were harvested and resuspended in growth medium to a concentration of 5×10^5 cells/mL. Cell suspension (100 μL) was added to a 96-well plate giving a total of 5×10^4 cells/well. The samples PeWN, PeWA and PeWB (100, 10 and 1 μg/mL final concentrations, 2 μL) were added. IFN-γ (100 U/mL, PeproTech Inc., Cranbury, NJ, USA) was added to the samples as a co-stimulant. Each sample was also added without co-stimulant, in a final concentration of 100 μg/mL. LPS (100 ng/mL, 1 μL, from *E. coli* 055:B5, Sigma-Aldrich) was included as positive control, with and without IFN-γ (0.1 U/μL). The plate was placed in a humid incubator with 5 % CO_2 at 37 °C for 20−22 hours. Supernatants were centrifuged for 2 min at 1400 rpm. To the isolated supernatants (50 μL), and standard solutions of NaNO (100, 50, 25, 12.5, 6.25, 3.13, 1.56, 0 μg/mL, 50 μL), were added Griess reagent A (1 % sulfanilamide in 5 % phosphoric acid, 50 μL) before incubation in the dark for 10 min. Then Griess reagent B (0.1 % *N*-(1-naphtyl) ethylenediamide, 50 μL) was added before absorbance reading at 530 nm. The experiment was carried out three times, in triplicates.

2.10. Cytokine detection

D2SC/1 cells were stimulated with samples (PeWN, PeWA and PeWB 100 μg/mL, 10 μg/mL) and controls (IFN-γ 100 U/mL, LPS 100 ng/mL w/wo IFN-γ, Pam3CSK4 100 μg/mL or 100 ng/mL, zymosan A 100 μg/mL or 10 μg/mL) as described in section 2.9, but with the total well volumes of 200 μL, and with 6 replicates for each condition. Supernatants (100 μL, three parallels x3) were collected and stored at -20 °C for 2–3 weeks, before analysis with mouse TNF-α, IL-6 and IL-12p70 DuoSet ELISA kits (Bio-Techne, Minneapolis, MN, USA), which were used as described by the manufacturer.

2.11. Statistical analysis

Data were expressed as the mean ± SD. Statistical analysis was performed, and graphs were drawn with GraphPad Prism v.8.0.1 (GraphPad Software, San Diego, CA, USA). Significance was determined using a one-way ANOVA with Dunnett's multiple comparisons test. $P < 0.05$ was considered statistically significant.

3. Results and discussion

3.1. Structural characterization of P. eryngii polysaccharide fractions

From the dried water extract PeW (3.3 % yield), three polysaccharide fractions were isolated after IEC; one neutral fraction, PeWN (20 % yield), and two acidic fractions PeWA and PeWB (12 and 40 % yield, respectively). The fractions were colorless, except for a brownish color of PeWB. The monosaccharide compositions obtained from methanolysis and subsequent GC analysis of the water extract, PeW, and the fractions, PeWN, PeWA and PeWB, are presented in Table 1. PeW contained large amounts of glucose (31 %), galactose (28 %), mannose (26 %) and 3-*O* methyl galactose (6 %). This is similar to what has been shown previously (Biscaia et al., 2017; Yan et al., 2019). Additionally, some uronic acids were present. PeWN contained glucose (31 %), galactose (28 %) and mannose (22 %), and 3-*O* methyl galactose (8 %) in similar ratios to the parenting fraction PeW. PeWA and PeWB contained more glucose (59–64 %), less galactose (9−7 %), and slightly less mannose (18−13 %) than PeWN. Glucuronic and galacturonic acid was present in these fractions in smaller amounts. SEC-MALLS analysis revealed that each fraction contained one major polymer population in terms of molecular size, as presented in Table 1. The three fractions contained polymers of weight-average molecular mass (M_w) of 16−23 kDa with low polydispersity. The linkage analysis data obtained by methylation and GC–MS analysis of the fractions are presented in Table 2. PeWN contained mainly (1→6)- and (1→2,6)-linked galactose. Most of the mannose was terminally linked, and might be attached to the *O*-2 of the galactose residues. The glucose residues were largely (1→3)-linked. Some terminally linked, and some (1→3,6)-, (1→4,6)-, and (1→6)-linked glucose was also observed. PeWA and PeWB contained more (1→3)-, (1→6)-, (1→3,6)- and terminally linked glucose, and (1→2) linked mannose.

Table 1
Monosaccharide compositions and total glycan content (w/w %) of the water extract, PeW, and fractions, PeWN, PeWA and PeWB, and weight-average molecular mass (M_w), polydispersity (M_w/M_n) of fractions PeWN, PeWA and PeWB from *P. eryngii*.

	Fuc	Xyl	Man	Gal	Glc	GlcA	GalA	3-O-Me Gal	Total glycan	M_w (kDa)	M_w/M_n
PeW	2	1	26	28	31	2	5	6	–	–	–
PeWN	1	<1	22	28	31	0	10	8	73	16.7	1.09
PeWA	0	0	18	9	59	4	8	3	53	22.8	1.08
PeWB	<1	1	13	7	64	6	5	3	61	17.2	1.31

Table 2
Relative abundance (% out of total) of linkage patterns detected in the water extract, PeW, and fractions, PeWN, PeWA, PeWB, from *P. eryngii*.

Linkage	PeW	PeWN	PeWA	PeWB
Xyl*p*-(1→	1	0	3	2
Fuc*p*-(1→	2	1	0	0
Glc*p*-(1→	8	10	14	14
→3)-Glc*p*-(1→	10	10	20	19
→3,6)-Glc*p*-(1→	3	3	6	6
→4)-Glc*p*-(1→	4	4	6	5
→6)-Glc*p*-(1→	7	4	10	14
→4,6)-Glc*p*-(1→	1	2	6	<1
Man*p*-(1→	23	11	16	13
→2)-Man*p*-(1→	2	1	8	6
→3)-Man*p*-(1→	0	8	2	2
→3,6)-Man*p*-(1→	0	1	1	1
Gal*p*-(1→	2	<1	<1	<1
→6)-Gal*p*-(1→	20	20	5	5
→2,6)-Gal*p*-(1→	17	18	5	5

3.1.1. 3-*O* methylated mannogalactan

The DEPT-135 edited HSQC NMR spectrum of the neutral fraction, PeWN, is presented in Fig. 2-A. The anomeric signals were readily assigned to the different monomers by comparison to results from the linkage analysis and reference spectra, such that the signals at 5.15/101.2 ppm and 5.01/100.6 ppm belong to H1/C1 on →2,6)-α-D-Gal*p*-(1→ (residue A) and →6)-α-D-Gal*p*-(1→ (residue C), respectively (Biscaia et al., 2017; Yan et al., 2019). The *O*-methyl groups were recognized as the correlations at 3.48/59.4 and 3.47/59.0 ppm in the HSQC spectrum, as shown previously (Abreu et al., 2021; Biscaia et al., 2017; Yan et al., 2019). These signals were also recognized in spectra reported by Xu et al. (2016) describing a *P. eryngii* mannogalactan. The *O*-methyl signals showed correlations in the HMBC (Fig. 2-B) and H2BC (not shown) spectra to H3/C3 (3.68/80.9 ppm; 3.57/81.7 ppm) on →2,6)-3-*O*Me-α-D-Gal*p*-(1→ (residue B) and →6)-3-*O*Me-α-D-Gal*p*-(1→ (residue D), demonstrating that the methyl groups are positioned on *O*-3 of galactose residues. This was further confirmed by correlations to H2/C2 (4.02/78.7 ppm; 3.89/70.2 ppm) on residues B and D respectively. The H2/C2 and H3/C3 signals of residues A and C were recognized through H2BC and HMBC correlations as presented in Table 3. Assignments of the ^{1}H and ^{13}C NMR spectra are also presented in Fig. 2-C and Fig. 2-D, respectively. Correlations could be found between H2 on residue C and the signal at 4.04 ppm, in the ROESY spectrum (not shown), which was assigned to H4 accordingly. ROESY correlation from this signal enabled the assignment of H5 as the peak at 4.21 ppm. Similar signals could be found for H4 and H5 on residue A, at 4.07 and 4.23 ppm, respectively. The former showed correlation to H2 in the HMBC spectrum, whereas the two shared a correlation in the ROESY spectrum. H4 on residue B showed ROESY correlations to the signal at 4.15 ppm, while H3 on residue D correlated with the 4.18 ppm, which was assigned to H5. HMBC correlations from H5/C5 on the different residues enabled the assignment of H6/C6 on all Gal*p* residues.

The anomeric signal of β-D-Man*p*-(1→ (residue E) was found at 4.81/104.3 ppm, indicating β-configuration as previously described (Biscaia et al., 2017; Yan et al., 2019). This signal showed HMBC correlations to H2/C2 on residue A, which confirmed the attachment at this position. Intraresidual correlations could also be found from H1/C1 to H2/C2 (4.12/73.34 ppm), between H2/C2 and H3/C3 (3.67/75.9 ppm), H3/C3 and H4/C4 (3.62/69.7 ppm), and H4/C4 and H5/C5 (3.40/79.1 ppm) in the H2BC spectrum. H6/C6 on residue E was recognized at 3.94/3.77 and 64.0 ppm through H2BC correlations to H5/C5 and HMBC correlations to H1/C1, H3/C3 and H4/C4. Some β-D-Man*p*-(1→ (residue F) were attached to residue B units. This was confirmed through an inter-residual HMBC correlation at 4.79 and 78.7 ppm, showing coupling between H1 on residue F and C2 on residue B. The remaining signals from residue F were assigned as shown in Table 3, and confirmed by correlations found in the COSY and DIPSI2 spectra. The suggested structure of the 3-*O* methylated mannogalactan is presented in Fig. 2-E; a partially 3-*O* methylated (1→6)-α-D-galactan with occasional α-mannose units at 2-*O* of both methylated and non-methylated galactose residues.

3.1.2. β-glucans

The DEPT-135 edited HSQC spectrum of fraction PeWA is presented in Fig. 3-A. Out of the β-glucan anomeric signals, the signal at 4.53/105.8 ppm was the most prominent, and was identified as H1/C1 of →6)-β-D-Glc*p*-(1→ (residue J). Comparison to reference spectra of YBG-S, a well-defined yeast derived β-glucan, enabled the identification of anomeric H1/C1 of other β-glucan residues: →3,6)-β-D-Glc*p*-(1→ (4.56/105.5 ppm; residue I), →3)-β-D-Glc*p*-(1→ (4.78/105.3 ppm; residue G), and terminally linked β-D-Glc*p*-(1→ (4.73/105.6 ppm; residue H) (Nyman et al., 2016, supplementary). The rest of each residue was readily identified through correlations found in the HMBC (Fig. 3-B) and H2BC spectra (not shown), as presented in Table 3. The assignments of ^{1}H and ^{13}C NMR signals are aslo presented in Fig. 3-C and 3-D, respectively. Intraresidual correlations could be found from H1/C1 of residue J to H2/C2 (3.35/75.9 ppm) and H6/C6 (4.22, 3.87/71.7 ppm) in the HMBC spectrum, the downfield shifted ^{13}C δ value of the latter confirming (1→6) linkage. H2/C2 correlated with the signal at 3.52 and 78.5 ppm, which was assigned H3/C3. This signal correlated with H4/C4 (3.47/72.5 ppm) in both HMBC and H2BC spectra. H4/C4 shared correlations with H5/C5 (3.64/77.8 ppm) and H6/C6. H3/C3 on residue I was identified at 3.76 and 87.5 ppm, through H2BC intraresidual correlations to both H2/C2 (3.54/75.6 ppm) and H4/C4 (3.54/77.8 ppm). H2/C2 also correlated with H1/C1 in the H2BC spectrum. H2/C2 (3.39/76.3 ppm) on residue H was identified through intraresidual correlations to H1/C1. HMBC correlations from H2/C2 to H3/C3 (3.55/78.5 ppm) and from H3/C3 to H4/C4 (3.43/72.6 ppm), and H2BC correlations between H3/C3 and H4/C4 enabled the identification of the remaining signals from residue H. The H2BC spectrum displayed intra-residual correlations from H1/C1 on residue G to H2/C2 (3.47/78.6 ppm).

Correlations from H1/C1 on residue H to H3/C3 on residues G and/or I in both HMBC and ROESY spectra indicate that the backbone of the structure is a (1→6)-β-D-glucan, with side-groups at *O*-3 of terminal β-D-Glc*p* and/or β-(1→3)-linked Glc*p* residues. The assignments were confirmed by correlations found in the COSY and DIPSI2 spectra. The suggested structure of the β-glucan is presented in Fig. 3-E.

3.1.3. Other glycans

In addition to the mannogalactan and β-glucans described previously, other glycan signals were identified through comparison to the linkage analysis results and reference spectra. An anomeric H1/C1

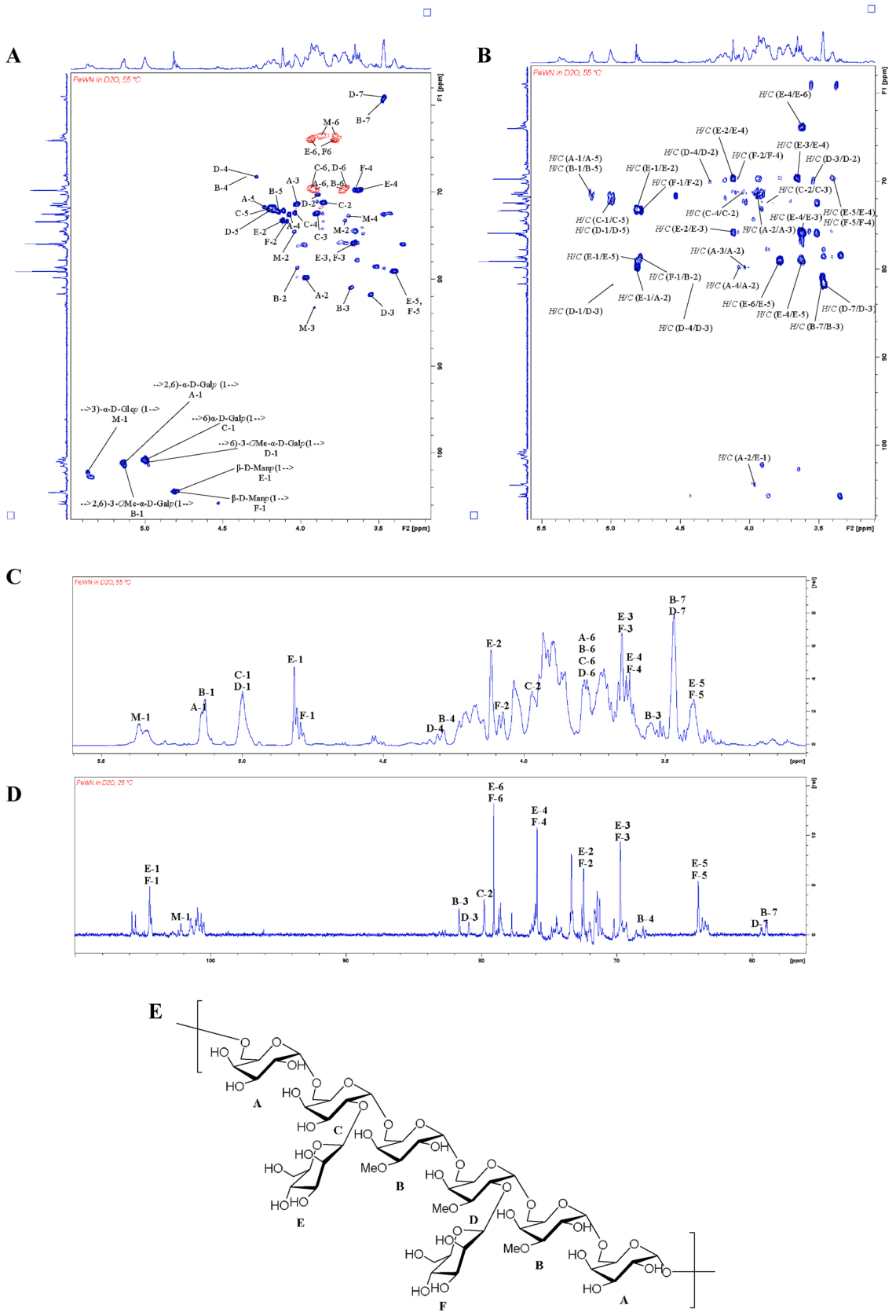

Fig. 2. NMR spectra of PeWN in D_2O, obtained at 55 °C on a Bruker Avance HD III 800 MHz spectrometer. **A.** DEPT-135 edited HSQC spectrum of PeWN. The spectrum shows markings of the different signals belonging to residues A-F of the partially methylated mannogalactan. **B.** HMBC spectrum of PeWN, showing inter- and intraresidual correlations of residuals A-F of the partially methylated mannogalactan. **C.** ^{1}H NMR spectrum. **D.** ^{13}C NMR spectrum. **E.** Suggested structure of partially methylated mannogalactan.

Table 3
Chemical shift assignments and correlations found in the NMR spectra of fractions PeWN and PeWA, assigned to a methylated mannogalactan (residues A-F), a (1-3)/(1-6)-β-D-glucan (residues G-J), a (1-2)-α-D-mannan (residues K-L) and a (1-3)-α-D-glucan (residue M). The samples were dissolved in D_2O, and spectra were recorded at 55 °C on a Bruker Avance III HD 800 MHz spectrometer. Spectra were referenced to 3-(trimethylsilyl) propionic 2,2,3,3-d_4 acid.

	Assigned monomer		δ 1H (ppm)	δ 13C (ppm)	HMBC correlations	H2BC correlations
A	→2,6)-α-D-Gal*p*-(1→	1	5.15	101.2	A-2, A-3, A-5	A-2
		2	3.97	79.8	A-1, A-3, A-4	A-1, A-3
		3	4.02	71.4	A-1, A-2, A-4	A-2
		4	4.07	72.5	A-2, A-3, A-5	A-3
		5	4.23	71.6	A-1, A-4, A-6	A-6
		6	3.93, 3.71	69.8	A-5	
B	→2,6)-α-D-(3-*O* Me) Gal*p*-(1→	1	5.13	101.4	B-5	B-2
		2	4.02	78.7		B-1, B-3
		3	3.68	80.9	B-2, B-4, B-7	B-2
		4	4.31	68.7	B-2, B-3	
		5	4.15	72.2	B-1	
		6	3.93, 3.71	69.8		
		7	3.48	59.4	B-3	
C	→6)-α-D-Gal*p*-(1→	1	5.01	100.6	C-2, C-3, C-4, C-5	C-2
		2	3.85	71.1	C-1	C-1, C-3
		3	3.9	72.5	C-1	C-2
		4	4.04	72.4	C-2	
		5	4.21	71.9	C-1, C-6	C-6
		6	3.93, 3.71	69.6	C-5	
D	→6)-α-D-(3-*O* Me) Gal*p*-(1→	1	5.01	100.6	D-3, D-5	
		2	3.85	71.1	D-3, D-4	D-3
		3	3.57	81.7	D-1, D-2, D-4, D-7	D-2
		4	4.29	68.3	D-2, D-3	
		5	4.18	72.0	D-1, D-6	D-6
		6	3.93, 3.71	69.6	D-5	
		7	3.47	59.0	D-3	
E	β-D-Man*p*-(1→	1	4.81	104.3	E-2, E-5, A-2	
		2	4.12	73.3	E-1, E-3, E-4	E-3
		3	3.67	75.9	E-2, E-4, E-5	E-2, E-4
		4	3.62	69.7	E-2, E-3, E-5	E-3, E-5
		5	3.40	79.1	E-1, E-3, E-4, E-6	E-4, E-6
		6	3.94, 3.77	64.0	E-5	E-5
F	β-D-Man*p*-(1→	1	4.79	104.3	F-2, B-2	
		2	4.09	73.4	F-1, F-3, F-4	
		3	3.67	75.9	F-2	
		4	3.65	69.7	F-2	
		5	3.40	79.1		
		6	3.94, 3.77	64.0		
G	→3)-β-D-Glc*p*-(1→	1	4.78	105.3	G-2	G-2
		2	3.58	75.9	G-1	G-1, G-3
		3	3.75	87.5	H-1, G-4	G-2, G-4
		4	3.54	71.1	G-3	G-3, G-5
		5	3.68	77.6	G-6	G-4
		6	3.87, 3.77	63.9	G-5	G-5
H	β-D-Glc*p*-(1→	1	4.74	105.6	G-3/I-3	H-2
		2	3.39	76.3	H-3	H-1
		3	3.55	78.5	H-2, H-4	H-4
		4	3.43	72.6	H-3	H-3, H-5
		5	3.46	78.8		H-4, H-6
		6	3.93, 3.75	63.7		H-5
I	→3,6)-β-D-Glc*p*-(1→	1	4.56	105.5	I-2	I-2
		2	3.54	75.6	I-1	I-1, I-3
		3	3.76	87.5	H-1, I-2	I-2, I-4
		4	3.59	71.1	I-5	I-3
		5	3.68	77.6	I-4	I-6
		6	4.22, 3.87	71.8		I-5
J	→6)-β-D-Glc*p*-(1→	1	4.53	105.8	J-2, J-6	J-2
		2	3.35	75.9	J-1, J-3	J-1, J-3
		3	3.52	78.5	J-2, J-4	J-2, J-4
		4	3.47	72.5	J-3, J-5, J-6	J-3, J-5
		5	3.64	77.8	J-4, J-6	J-4, J-6
		6	4.22, 3.87	71.7	J-1, J-4, J-5	J-5
K	→2)-α-D-Man*p*-(1→	1	5.28	103.4	K-2, K-3, K-5	
		2	4.12	81.1	K-1, L-1	
		3	3.75	76.1	K-1	
		4	3.69	69.9		
		5	3.95	73.0	K-1	
		6	3.89, 3.75	63.8		
L	α-D-Man*p*-(1→	1	5.07	104.9	L-3, L-5, K-2	
		2	–	–		
		3	3.75	76.1	L-1	
		4	3.69	69.9		
		5	3.85	73.3	L-1	
		6	3.89, 3.75	63.8		
M	→3)-α-D-Glc*p*-(1→	1	5.37	102.2		
		2	3.71	73.3		
		3	3.91	83.3		
		4	3.69	72.7		
		5	4.04	74.6		
		6	3.87, 3.78	63.4		

‘Additional correlations were found in COSY, DIPSI2 and ROESY spectra.

signal was found at 5.38 and 102.3 ppm in the HSQC spectrum of PeWN (Fig. 4-A), correlating such that the remaining signals were identified at 3.69/72.7 ppm (H2/C2), 3.91/83.3 ppm (H3/C3), 3.72/73.3 ppm (H4/C4), 4.04/74.5 ppm (H5/C5), and 3.86 & 3.78/63.5 ppm (H6/C6). These signals corresponded to reference spectra of nigeropentaose, a pentamer of →3)-α-D-Glc*p*-(1→ (Megazyme Ltd., Bray, Ireland, HSQC spectrum available in supplementary data). This is also in accordance with spectra published recently by Abreu et al. (2021), describing a linear (1→3)-α-D-glucan from *P. eryngii*, found in association with a methylated mannogalactan and β-glucans.

Anomeric signals at 5.07/104.9 ppm and 5.28/103.4 ppm in the HSQC spectrum of PeWA (Fig. 4-B are suggested to belong to α-D-Man*p*-(1→ and →2)-α-D-Man*p*-(1→ respectively, with H2/C2 on the →2)-α-D-Man*p*-(1→ residues visible at 4.12/81.1 ppm. This is based on spectra of a previously reported (1→6)-α-D-mannan with occasional (1→2)-linked residues (Nyman et al., 2016). Some HMBC correlations were found to support this, as presented in Table 3.

To summarize, fractions PeWN, PeWA and PeWB all contain some mannogalactan. PeWN contains mostly mannogalactan and is thus quite similar to the previously described partially methylated mannogalactans, both in M_w and structure (Biscaia et al., 2017; Yan et al., 2019). In addition, PeWA and PeWB contain significant amounts of (1→3)/(1→6)-β-D-glucan. Spectra of PeWA and PeWB (not shown) were almost identical; PeWB having additional signals outside the carbohydrate region and a brownish color, indicating the presence of non-polysaccharide components in this fraction.

3.2. Activity studies

3.2.1. HEK-Blue™ binding assays

To assess the activity of the water-soluble *P. eryngii* polysaccharides towards TLR2 and dectin-1, a series of experiments were performed on TLR2, TLR2-TLR6 and dectin-1 transfected HEK cells, as well as on control parental null cells. These cells express the relevant human receptor gene in addition to a reporter gene leading to the secretion of SEAP when nuclear factor-κB (NF-κB) pathways are activated. By using a SEAP detecting reagent this activation is monitored and analyzed by

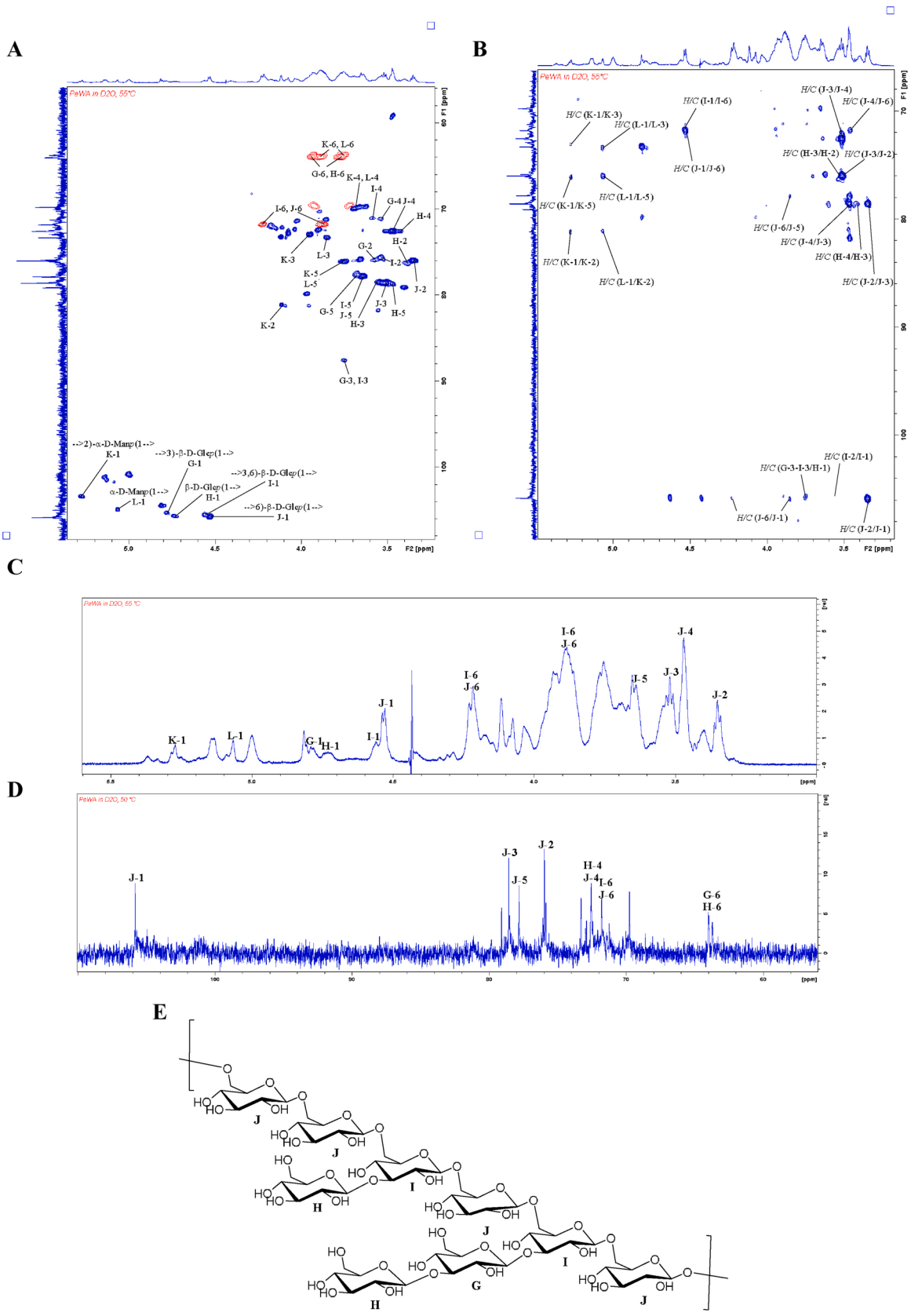

Fig. 3. NMR spectra of PeWA in D_2O, obtained at 55 °C on a Bruker Avance HD III 800 MHz spectrometer. **A.** DEPT-135 edited HSQC spectrum of PeWA. The spectrum shows markings of the different signals belonging to residues G-J on the β-glucan. **B.** HMBC spectrum of PeWA, showing inter- and intraresidual correlations of residues G-J. **C.** ^{1}H NMR spectrum. **D.** ^{13}C NMR spectrum. **E.** Suggested structure of β-glucan.

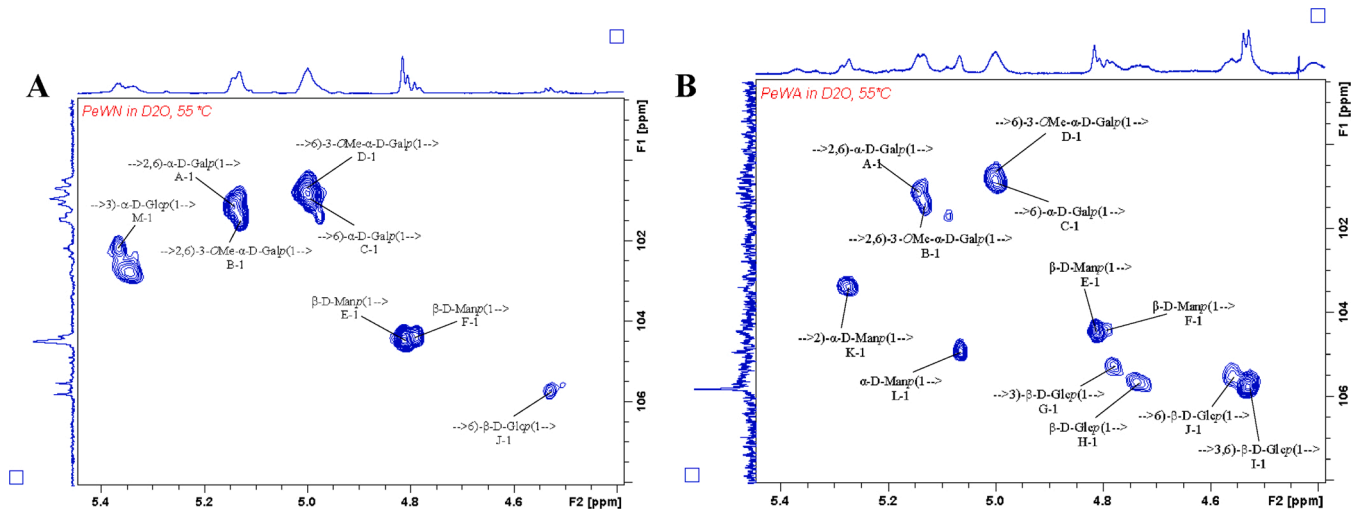

Fig. 4. Anomeric regions of the HSQC spectra of **A** PeWN and **B** PeWA. Samples dissolved in D_2O, and spectra obtained at 55 °C on a Bruker Avance HD III 800 MHz spectrometer.

absorbance reading. The lipopeptides Pam2CSK4 and Pam3CSK4, which possess two and three palmitoyl chains, and which are known to bind to TLR2-TLR6 and TLR2-TLR1 respectively, were included as controls to all assays. Zymosan A and zymosan depleted were also included, as both bind dectin-1, but only zymosan A bind TLR2-TLR6 (Ikeda et al., 2008). LPS was included to ensure lack of TLR4 expression, and laminarin was added as a control of dectin-1 activity (Brown & Gordon, 2001). TNF-α was used as a positive control for the direct activation of NF-κB pathways in the parental cell line HEK-Blue™ Null1.

The results from the TLR2 binding assay are presented in Fig. 5-A. Surprisingly, PeWN, which is the most mannogalactan-rich fraction, did not activate TLR2. This is opposite to results reported by Yan et al. (2019). In their study, pretreatment with TLR2-blocking antibodies, or with the TLR2 inhibitor C29, lead to a decrease in TNF-α and IL-6 production by RAW264.7 macrophages, indicating that the mannogalactan activated TLR2. As with PeWN, PeWA showed no sign of binding, while

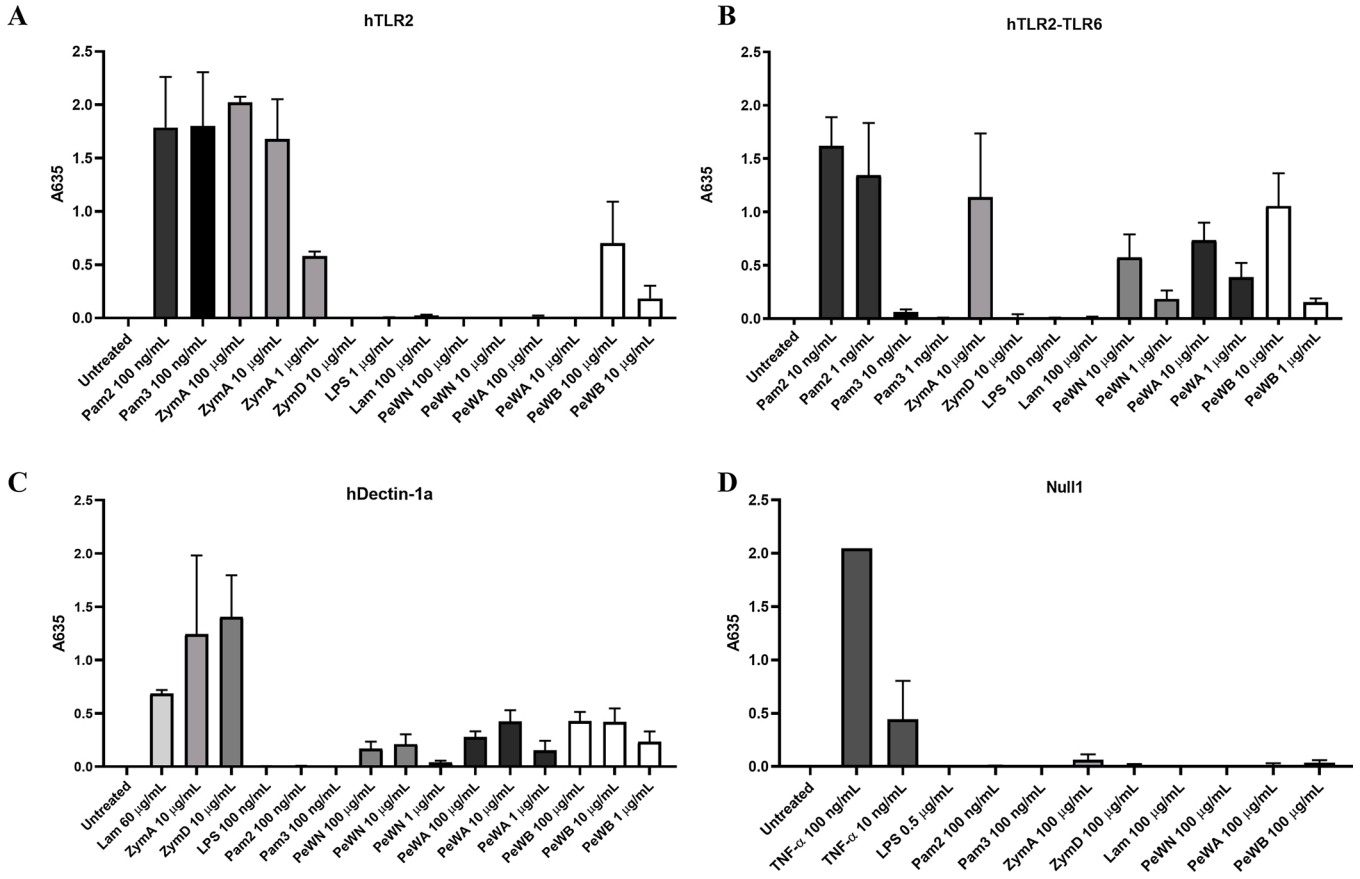

Fig. 5. Activation of HEK-Blue™ cells (absorbance at 635 nm) after incubation with *P. eryngii* fractions (PeWN, PeWA, PeWB) and controls, adjusted for background activity from untreated cells. **A.** HEK-Blue™ hTLR2. **B.** HEK-Blue™ hTLR2-TLR6. **C.** HEK-Blue hDectin-1a. **D.** HEK-Blue™ null1 cells. Error bars represents the SD of three series of experiments. Pam2 = Pam2CSK4 lipopeptide; Pam3 = Pam3CSK 4 lipopeptide, ZymA = zymosan A; ZymD = zymosan depleted; Lam = laminarin.

PeWB was able to activate the cells. The lack of binding by PeWA compared to PeWB despite their structural similarities indicate that other co-eluted compounds in PeWB are involved in the activation, rather than the polysaccharides. The difference in color of the two samples supports this, as this strongly suggests the presence of other, non-polysaccharide residues in PeWB.

The reporter cell line HEK-Blue™ hTLR2 expresses, in addition to high levels of TLR2, endogenous levels of TLR1 and TLR6, thus enabling the activation through either TLR2-TLR1 or TLR2-TLR6. In order to determine which of the two heterodimers were involved, a similar experiment was conducted using HEK-Blue™ hTLR2-TLR6 cells. The results, presented in Fig. 5-B, show that PeWB binds and activates TLR2-TLR6 at 1−10 μg/mL, indicating that the TLR2 activation is initiated by binding to the TLR2-TLR6 heterodimer. Still, because of the results from the TLR2 binding assay, this activity is likely caused by non-polysaccharide residues.

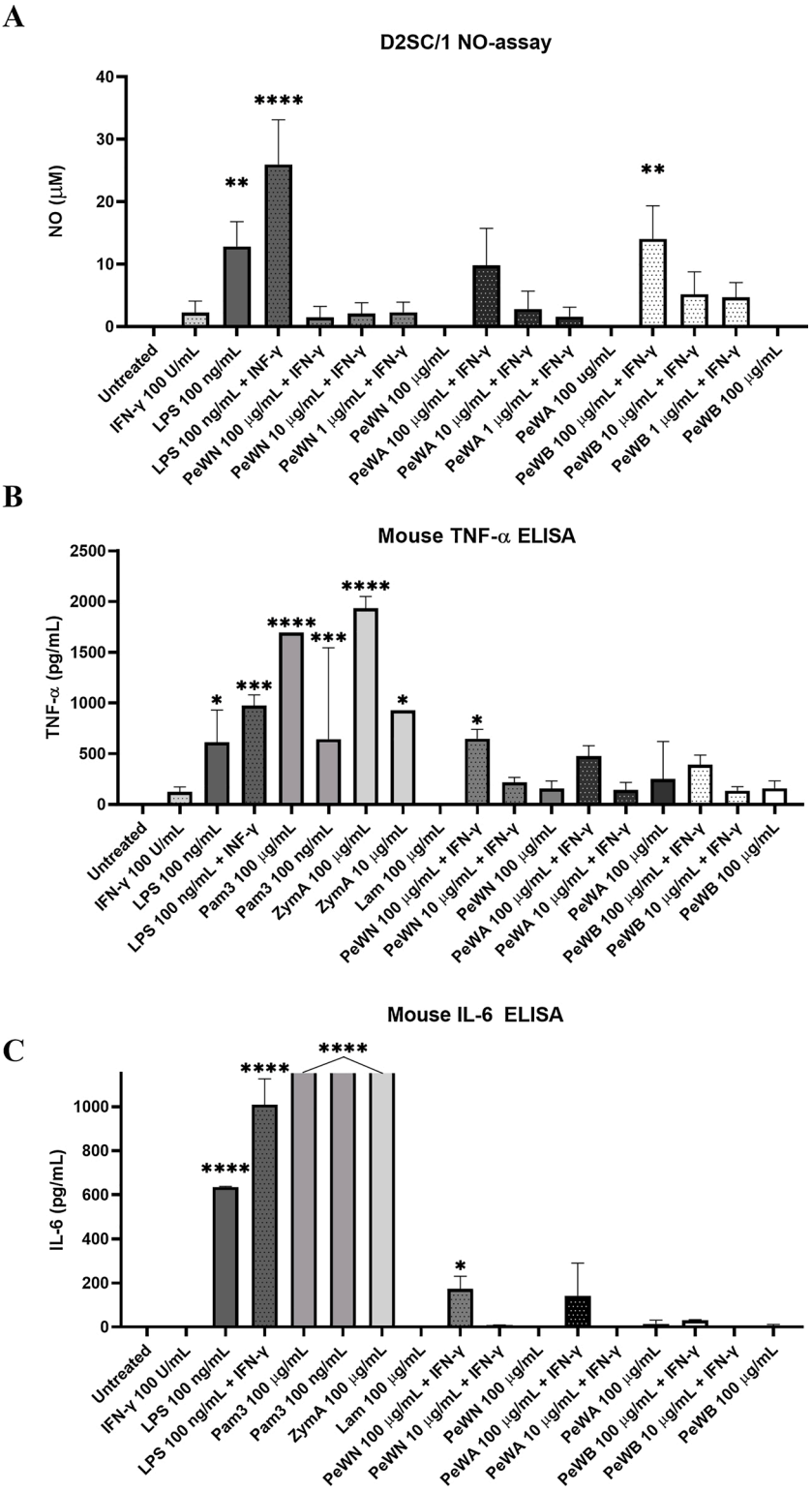

Fig. 6. Activation of D2SC/1 cells after incubation with *P. eryngii* fractions (PeWN, PeWA and PeWB) and controls, adjusted for background activity from untreated cells and statistically compared to cells treated with IFN-γ (100 U/mL). **A** Production of nitric oxide (NO). **B** Production of tumor necrosis factor-α (TNF-α). **C** Production of interleukin (IL) 6, (Pam3 and ZymA values above accurate range). Error bars represents the SD of three series of experiments (IL-6 = two series). * $p < 0.0332$, ** $p < 0.0021$, *** $p < 0.0002$, **** $p < 0.0001$. Pam3 = Pam3CSK4 lipopeptide; ZymA = zymosan A; Lam = laminarin.

NMR analysis demonstrated that all fractions contain β-glucan, which is why a similar experiment was carried out on HEK-Blue™-hDectin-1a cells (Fig. 5-C). Some activation was detected after incubation with each of the three fractions, and slightly more with PeWA and PeWB than with PeWN. This is consistent with the higher β-glucan content of these samples. The soluble (1→3)-linked linear β-glucan laminarin was also able to activate dectin-1, along with the particulate β-glucans zymosan A and zymosan depleted. This further strengthens the theory that both soluble and particulate β-glucans are able to activate human dectin-1 (Takano et al., 2017). In contrast, Vetvicka et al. (2019) reported that *P. eryngii* glucans inhibited dectin-1 on mouse RAW264.7 macrophages, which is consistent with the theorized inter-species differences. The parental cell line responded only to the positive control TNF-α (Fig. 5-D), demonstrating that no other receptors present on the HEK cells were involved in the activation.

3.2.2. Activation of dendritic D2SC/1 cells

Nitric oxide (NO) is often produced by macrophages and DC upon activation, and NO production is a marker of a proinflammatory phenotype in these cells (Müller et al., 2017). As such, we wanted to test if the *P. eryngii* polysaccharide fractions were able to activate D2SC/1 cells, by using the Griess assay to measure NO levels in cell supernatants. Experiments were conducted with and without IFN-γ, since TLR-mediated NO-production normally depends on the presence of INF-γ together with the ligand (Müller et al., 2017). The exception is TLR4, which is activated both by LPS alone and synergistically with IFN-γ present (Müller et al., 2017). As such, production of NO in the absence of IFN-γ indicates TLR4 activation, which in turn may be a sign of LPS contamination. The results in Fig. 6-A showed that none of the samples were able to induce NO-production without IFN-γ present, indicating absence of IFN-γ independent activation, and thus minimum LPS contamination. Cells stimulated with LPS in the absence of IFN-γ produced statistically significant amounts of NO, showing that the cells could respond to LPS when present. The NO-production induced by PeWN and PeWA in combination with IFN-γ was not significantly different from the IFN-γ control. This is in accordance with the lack of TLR-2 activity observed from these two fractions. PeWB at the highest concentration (100 μg/mL) was the only fraction able to increase NO-production significantly compared to IFN-γ-treated cells (Fig. 6-A).

Mannogalactans from *P. eryngii* have previously been reported to induce NO-production in human (THP-1) and mouse (RAW264.7) macrophages in the absence of IFN-γ (Abreu et al., 2021; Xu et al., 2016; Yan et al., 2019). These results are not in accordance with the present study where the mannogalactan rich fraction PeWN was unable to induce NO-production. In studies where activities are solely determined without addition of IFN-γ, and other attempts to detect or quantify LPS activity (de Santana-Filho et al., 2012; Govers et al., 2016; Novitsky, 1998) are not conducted, one cannot out-rule false positive results caused by LPS contamination. Yan et al. (2019) did perform measures to remove LPS by treatment with polymyxin B but did not identify the receptor involved in the NO-production.

Production of the proinflammatory cytokines TNF-α, IL-6 and IL-12p70 by mouse dendritic cells stimulated with fractions PeWN, PeWA and PeWB was measured using ELISA kits. As shown in Fig. 6-B and -C, all three samples induced some TNF-α and IL-6 production when combined with IFN-γ, showing a synergistic effect. None of the samples induced a statistically significant amount of TNF-α when compared to IFN-γ, although there seemed to be some amount produced under each of the conditions containing 100 μg/mL sample and IFN-γ. IL-6 was produced in smaller amounts. PeWN (100 μg/mL) with IFN-γ induced a statistically significant production of IL-6 compared to IFN-γ stimulated cells. The controls Pam3CSK4 and zymosan A induced an IL-6 production above the accurate range of the assay, and values are thus less reliable. The cells did not produce IL-12p70 after stimulation with any of the samples or controls.

Previously, *P. eryngii* polysaccharides have been found to induce production of TNF-α, IL-1β, IL-6 and IL-10 (Abreu et al., 2021; Xu et al., 2016; Yan et al., 2019). The present results are in accordance with the mentioned data, although the amounts produced seems to vary. In general, the cytokine levels detected in the present study are below what has previously been reported. This may be due to the use of different cell lines from different species, as the previously published data all use macrophages, while dendritic cells are used herein, and both human and mouse cells have been used in the various studies. The observed differences may nevertheless indicate that the activity of water-soluble *P. eryngii* polysaccharides is less prominent than previously suggested.

4. Conclusion

This study has shown that king oyster mushroom, *P. eryngii*, contains a partially 3-*O* methylated (1→6)-linked α-D-galactan with occasional β-D-mannose units at 2-*O* on both methylated and non-methylated galactose residues. Additionally, (1→3)/(1→6)-β-D-glucans, traces of a (1→3)-α-D-glucan and a (1→2)-α-D-mannan were identified in the water-soluble fractions. Contradictory to previous reports, the methylated mannogalactan-rich fraction PeWN could not bind to TLR2 nor induce NO production in DCs. However, PeWN did induce production of minor amounts of TNF-α and IL-6 in DCs. Fractions containing higher amounts of β-glucan (PeWA and PeWB), showed some activity towards both TLR2-TLR6 and dectin-1, and induced NO-production in mouse-derived DCs. The β-glucans are believed to be responsible for the dectin-1 activity, while activity towards TLR2, and thereby TLR2-TLR6, is likely caused by non-carbohydrate components. Taken together, these data suggests that although the water-soluble *P. eryngii* polysaccharides are active towards the mentioned systems, the activity is modest. Our results also demonstrate the importance of a thorough characterization and purification of water-soluble polysaccharide fractions in order to confirm their biological activity.

CRediT authorship contribution statement

Christiane Færestrand Ellefsen: Investigation, Formal analysis, Writing - original draft, Visualization. **Christian Winther Wold:** Investigation, Methodology. **Alistair L. Wilkins:** Methodology, Software. **Frode Rise:** Methodology, Software. **Anne Berit C. Samuelsen:** Methodology, Supervision, Conceptualization, Writing - review & editing.

Acknowledgements

The authors thank Prof. Klaus Høiland, Department of Biosciences University of Oslo for *P. eryngii* identification, Hanne Zobel, NOFIMA Food Research Institute and Hoai Thi Nguyen Aas, Department of Pharmacy for technical assistance. This work was partly supported by the Research Council of Norway through the Norwegian NMR Platform, NNP (226244/F50). Additional support by the Department of Chemistry and the Faculty of Mathematics and Natural Sciences at University of Oslo is also acknowledged.

Appendix A. Supplementary data

Supplementary material related to this article can be found, in the online version, at doi:https://doi.org/10.1016/j.carbpol.2021.117991.

References

Abreu, H., Zavadinack, M., Smiderle, F. R., Cipriani, T. R., Cordeiro, L. M. C., & Iacomini, M. (2021). Polysaccharides from *Pleurotus eryngii*: Selective extraction methodologies and their modulatory effects on THP-1 macrophages. *Carbohydrate Polymers, 252*, Article 117177.

Barbosa, J. R., dos Santos Freitas, M. M., da Silva Martins, L. H., & de Carvalho, R. N., Junior (2020). Polysaccharides of mushroom *Pleurotus* spp.: New

extraction techniques, biological activities and development of new technologies. *Carbohydrate Polymers, 229*, Article 115550.
Baysal, E., Peker, H., Yalinkilic, M. K., & Temiz, A. (2003). Cultivation of oyster mushroom on waste paper with some added supplementary materials. *Bioresource Technology, 89*, 95–97.
Biscaia, S. M. P., Carbonero, E. R., Bellan, D. L., Borges, B. S., Costa, C. R., Rossi, G. R., et al. (2017). Safe therapeutics of murine melanoma model using novel antineoplastic, the partially methylated mannogalactan from *Pleurotus eryngii*. *Carbohydrate Polymers, 178*, 95–104.
Bose, N., Chan, A. S. H., Guerrero, F., Maristany, C. M., Qiu, X., Walsh, R. M., et al. (2013). Binding of soluble yeast β-glucan to human neutrophils and monocytes is complement-dependent. *Frontiers in Immunology, 4*, 230.
Brown, G. D., & Gordon, S. (2001). A new receptor for β-glucans. *Nature, 413*, 36–37.
Brown, G. D., Herre, J., Williams, D. L., Willment, J. A., Marshall, A. S. J., & Gordon, S. (2003). Dectin-1 mediates the biological effects of β-Glucans. *The Journal of Experimental Medicine, 197*(9), 1119–1124.
Bruggen, R. V., Drewniak, A., Jansen, M., Houdt, M. V., Roos, D., Chapel, H., et al. (2009). Complement receptor 3, not Dectin-1, is the major receptor on human neutrophils for β-glucan-bearing particles. *Molecular Immunology, 47*, 575–581.
Carbonero, E. R., Gracher, A. H. P., Smiderle, F. R., Rosado, F. R., Sassaki, G. L., Gorin, P. A. J., et al. (2006). A β-glucan from the fruit bodies of edible mushroom *Pleurotus eryngii* and *Pleurotus ostreatoroseus*. *Carbohydrate Polymers, 66*, 252–257.
Carbonero, E. R., Gracher, A. H. P., Rosa, M. C. C., Torri, G., Sassaki, G. L., Gorin, P. A. J., et al. (2008). Unusual partially 3-*O*-methylated α-galactan from mushrooms of the genus *Pleurotus*. *Phytochemistry, 69*, 252–257.
de Santana-Filho, A. P., Noleto, G. R., Gorin, P. A. J., de Souza, L. M., Iacomini, M., & Sassaki, G. L. (2012). GC-MS detection and quantification of lipopolysaccharides in polysaccharides through 3-O-acetyl fatty acid methyl esters. *Carbohydrate Polymers, 87*, 2730–2734.
Di Carlo, F. J., & Fiore, J. V. (1958). On the composition of Zymosan. *Science, 127*(3301), 756–757.
DuBois, M., Gilles, K. A., Hamilton, J. K., Rebers, P. A., & Smith, F. (1956). Colorimetric method for determination of sugars and related substances. *Analytical Chemistry, 28*(3), 350–356.
Ferwerda, G., Meyer-Wentrup, F., Kullberg, B. J., Netea, M. G., & Adema, G. J. (2008). Dectin-1 synergizes with TLR2 and TLR4 for cytokine production in human primary monocytes and macrophages. *Cellular Microbiology, 10*, 2058–2066.
Gantner, B. N., Simmons, R. M., Canavera, S. J., Akira, S., & Underhill, D. M. (2003). Collaborative induction of inflammatory responses by Dectin-1 and toll-like receptor 2. *The Journal of Experimental Medicine, 197*(9), 1107–1117.
Goodridge, H. S., Reyes, C. N., Becker, C. A., Katsumoto, T. R., Ma, J., Wolf, A. J., et al. (2011). Activation of the innate immune receptor Dectin-1 upon formation of a "phagocytic synapse". *Nature, 472*(7344), 471–475.
Govers, C., Tomassen, M. M. M., Rieder, A., Ballance, S., Knutsen, S. H., & Mes, J. J. (2016). Lipopolysaccharide quantification and alkali-based inactivation in polysaccharide preparations to enable *in vitro* immune modulatory studies. *Bioactive Carbohydrates and Dietary Fibre, 8*, 15–25.
Hohl, T. M., Rivera, A., & Pamer, E. G. (2006). Immunity to fungi. *Current Opinion in Immunology, 18*, 465–472.
Hong, F., Yan, J., Baran, J. T., Allendorf, D. J., Hansen, R. D., Ostroff, G. R., et al. (2004). Mechanism by which orally administered *β*-1,3-Glucans enhance the tumoricidal activity of antitumor monoclonal antibodies in murine tumor models. *The Journal of Immunology, 173*, 797–806.
Ikeda, Y., Adachi, Y., Ishii, T., Miura, N., Tamura, H., & Ohno, N. (2008). Dissociation of toll-like receptor 2-mediated innate immune response to zymosan by organic solvent-treatment without loss of dectin-1 reactivity. *Biological & Pharmaceutical Bulletin, 31*(1), 13–18.
Ma, G., Yang, W., Mariga, A. M., Fang, Y., Ma, N., Pei, F., et al. (2014). Purification, characterization and antitumor activity of polysaccharides from *Pleurotus eryngii* residue. *Carbohydrate Polymers, 114*, 297–305.
Medzhitov, R., & Janeway, C., Jr. (2000). Innate immune recognition: Mechanisms and pathways. *Immunological Reviews, 173*, 89–97.
Müller, E., Christopoulos, P. F., Halder, S., Lunde, A., Beraki, K., Speth, M., et al. (2017). Toll-like receptor ligands and Interferon-γ synergize for induction of antitumor M1 macrophages. *Frontiers in Immunology, 8*(1383).
Murphy, K., & Weaver, C. (2017). *Janeway's immunobiology* (9th ed.). New York: Garland Science/Taylor & Francis (Chapter 3).
Novitsky, T. J. (1998). Limitations of the Limulus amebocyte lysate test in demonstrating circulating lipopolysaccharides. *Annals of the New York Academy of Sciences, 851*, 416–421.
Nyman, A. A. T., Aachmann, F. L., Rise, F., Ballance, S., & Samuelsen, A. B. C. (2016). Structural characterization of a branched (1→6)-α-mannan and β-glucans isolated from the fruiting bodies of *Cantharellus cibarius*. *Carbohydrate Polymers, 146*, 197–207.
Ozinsky, A., Underhill, D. M., Fontenot, J. D., Hajjar, A. M., Smith, K. D., Wilson, C. B., et al. (2000). The repertoire for pattern recognition of pathogens by the innate immune system is defined by cooperation between Toll-like receptors. *Proceedings of the National Academy of Sciences of the United States of America, 97*(25), 13766–13771.
Pettolino, F. A., Walsh, C., Fincher, G. B., & Bacic, A. (2012). Determining the polysaccharide composition of plant cell walls. *Nature Protocols, 7*(9), 1590–1607.
Rock, F. L., Hardiman, G., Timans, J. C., Kastelein, R. A., & Bazan, J. F. (1998). A family of human receptors structurally related to *Drosophila* toll. *Proceedings of the National Academy of Sciences of the United States of America, 95*(2), 588–593.
Rosado, F. R., Carbonero, E. R., Claudino, R. F., Tischer, C. A., Kemmelmeier, C., & Iacomini, M. (2003). The presence of partially 3-*O*-methylated mannogalactan from fruit bodies of edible basidiomycetes *Pleurotus ostreatus 'florida'* Berk. and *Pleurotus ostreatoroseus* Sing. *FEMS Microbiology Letters, 221*, 119–124.
Silveira, M. L. L., Smiderle, F. R., Agostini, F., Pereira, E. M., Bonatti-Chaves, M., Wisbeck, E., et al. (2015). Exopolysaccharide produced by *Pleurotus sajor-caju*: Its chemical structure and anti-inflammatory activity. *International Journal of Biological Macromolecules, 75*, 90–96.
Smiderle, F. R., Olsen, L. M., Carbonero, E. R., Marcon, R., Baggio, C. H., Freitas, C. S., et al. (2008). A 3-*O*-methylated mannogalactan from *Pleurotus pulmonarius*: Structure and antinociceptive effect. *Phytochemistry, 69*, 2731–2736.
Synytsya, A., Míckova, K., Synytsya, A., Jablonský, I., Spevácek, J., Erban, V., et al. (2009). Glucans from fruit bodies of cultivated mushrooms *Pleurotus ostreatus* and *Pleurotus eryngii*: Structure and potential prebiotic activity. *Carbohydrate Polymers, 76*, 548–556.
Takano, T., Motozono, C., Imai, T., Sonoda, K.-H., Nakanishi, Y., & Yamasaki, S. (2017). Dectin-1 intracellular domain determines species-specific ligand spectrum by modulating receptor sensitivity. *The Journal of Biological Chemistry, 292*(41), 16933–16941.
Takeuchi, O., Kawai, T., Mühlradt, P. F., Morr, M., Radolf, J. D., Zychlinsky, A., et al. (2001). Discrimination of bacterial lipoproteins by Toll-like receptor 6. *International Immunology, 13*(7), 933–940.
Takeuchi, O., Sato, S., Horiuchi, T., Hoshino, K., Takeda, K., Dong, Z., et al. (2002). Cutting edge: Role of toll-like receptor 1 in mediating immune response to microbial lipoproteins. *The Journal of Immunology, 169*, 10–14.
Vetvicka, V., Gover, O., Karpovsky, M., Hayby, H., Danay, O., Ezov, N., et al. (2019). Immune-modulating activities of glucans extracted from *Pleurotus ostreatus* and *Pleurotus eryngii*. *Journal of Functional Foods, 54*, 81–91.
Willcocks, S., Offord, V., Seyfert, H.-M., Coffey, T. J., & Werling, D. (2013). Species-specific PAMP recognition by TLR2 and evidence for species-restricted interaction with Dectin-1. *Journal of Leukocyte Biology, 94*, 449–458.
Willment, J. A., Marshall, A. S. J., Reid, D. M., Williams, D. L., Wong, S. Y. C., Gordon, S., et al. (2005). The human β-glucan receptor is widely expressed and functionally equivalent to murine Dectin-1 on primary cells. *European Journal of Immunology, 35*, 1539–1547.
Xu, D., Wang, H., Zheng, W., Gao, Y., Wang, M., Zhang, Y., et al. (2016). Characterization and immunomodulatory activities of polysaccharide isolated from *Pleurotus eryngii*. *International Journal of Biological Macromolecules, 92*, 30–36.
Yadav, M., & Schorey, J. S. (2006). The β-glucan receptor dectin-1 functions together with TLR2 to mediate macrophage activation by mycobacteria. *Blood, 209*(9), 3168–3175.
Yan, J., Meng, Y., Zhang, M., Zhou, X., Cheng, H., Sun, L., et al. (2019). A 3-O-methylated heterogalactan from *Pleurotus eryngii* activates machrophages. *Carbohydrate Polymers, 206*, 706–715.
Zervakis, G. I., Venturella, G., & Papadopoulou, K. (2001). Genetic polymorphism and taxonomic infrastructure of the *Pleurotus eryngii* species-complex as determined by RAPD analysis, isozyme profiles and ecomorphological characters. *Microbiology, 147*, 3183–3194.
Zhang, B., Li, Y., Zhang, F., Linhardt, R. J., Zeng, G., & Zhang, A. (2020). Extraction, structure and bioactivities of the polysaccharides from *Pleurotus eryngii*: A review. *International Journal of Biological Macromolecules, 150*, 1342–1347.
Zhang, A., Xu, M., Fu, L., & Sun, P. (2013). Structural elucidation of a novel mannogalactan isolated from the fruiting bodies of *Pleurotus geesteranus*. *Carbohydrate Polymers, 92*, 236–240.
Zhang, A., Zhang, Y., Yang, J., & Sun, P. (2013). Structural elucidation of a novel heteropolysaccharide from fruiting bodies of *Pleurotus eryngii*. *Carbohydrate Polymers, 92*, 2239–2240.